Crystal structure and Hirshfeld surface analysis of {2-[bis(pyridin-2-ylmethyl)amino]ethane-1-thiolato}chloridocadmium(II)

Todd M. Reynolds, Steven M. Berry‡ and Deborah C. Bebout*

Department of Chemistry, William & Mary, Williamsburg, VA 23187-8795, USA. *Correspondence e-mail: dcbebo@wm.edu

The title compound, $[Cd(C_{14}H_{16}N_3S)Cl]$ or [CdLCl] (1), where LH = 2-[bis(pyridin-2-ylmethyl)amino]ethane-1-thiol, was prepared and structurally characterized. The Cd^{2+} complex crystallizes in $P2_1/c$ with a distorted trigonal–bipyramidal metal coordination geometry. Supramolecular interactions in 1 include parallel offset face-to-face interactions between inversion-related pyridyl rings and potential hydrogen bonds with chlorine or sulfur as the acceptor. Additional cooperative pyridyl–pyridyl interactions with roughly 45° tilt angles and centroid–centroid distances of less than 5.5 Å likely also contribute to the overall solid-state stability. Hirshfeld surface analysis indicates that H⋯H (51.2%), Cl⋯H/H⋯Cl (13.9%), C⋯H/H⋯C (12.3%) and S⋯H/H⋯S (11.8%) interactions are dominant in the solid state.

1. Chemical context

The cambialistic ζ-class of carbonic anhydrases from marine diatoms relying on Cd^{2+} as their metal cofactor when Zn^{2+} is scarce were discovered in 2000 (Lane & Morel, 2000). These proteins have His_2Cys metal-binding environments like the prokaryotic β-class of Zn^{2+}-dependent carbonic anhydrases (Xu et al., 2008). Despite the concurrence of histidine and cysteine in the active site of these proteins associated with the only known physiologically beneficial role for Cd^{2+}, structurally characterized complexes of Cd^{2+} with chelating ligands containing a combination of aromatic amine and alkylthiolate donors remain rare (CSD, Version 5.45, update of June 2024; Groom et al., 2016) and include only multinuclear complexes (Sturner et al., 2024; Brennan et al. 2022; Lai et al. 2013). Herein, the preparation, crystal structure and Hirshfeld surface analysis of mononuclear {2-[bis(pyridin-2-ylmethyl)amino]ethane-1-thiolato}chloridocadmium(II) are reported.
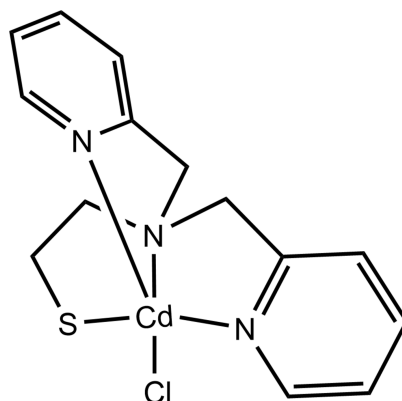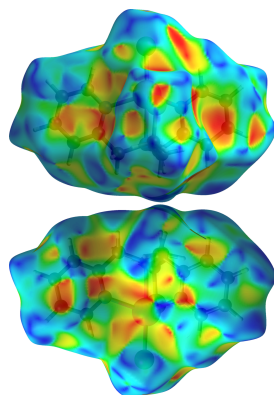
Table 1
Selected geometric parameters (Å, °) for **1**.

Cd1—N1A	2.3313 (11)	Cd1—S1	2.4710 (4)
Cd1—N1B	2.3151 (11)	Cd1—Cl1	2.4674 (4)
Cd1—N1	2.4758 (11)		
N1A—Cd1—N1B	110.87 (4)	N1B—Cd1—S1	116.16 (3)
N1A—Cd1—N1	71.91 (4)	N1B—Cd1—Cl1	100.00 (3)
N1A—Cd1—S1	113.78 (3)	S1—Cd1—N1	82.51 (3)
N1A—Cd1—Cl1	97.67 (3)	Cl1—Cd1—N1	161.29 (3)
N1B—Cd1—N1	70.70 (4)	Cl1—Cd1—S1	116.159 (13)

Table 2
Overview of pyridyl–pyridyl ring geometry interaction metrics (Å, °) for **1**.

$Cg1$ and $Cg2$ are the centroids of the N1A/C1A–C5A and N1B/C1B–C5B rings, respectively.

Centroids	Dihedral angle between rings	Centroid–centroid distance	Centroid–plane distance	Slippage
$Cg1\cdots Cg1^i$	48.66 (7)	5.3780 (6)	1.9060 (6)	–
$Cg1\cdots Cg1^{ii}$	0	4.1803 (5)	3.6544 (6)	2.030
$Cg2\cdots Cg1^{ii}$	45.41 (4)	4.9435 (5)	2.0400 (5)	–
$Cg2\cdots Cg2^{iii}$	0	3.4649 (4)	3.3629 (5)	0.834

Symmetry codes: (i) $1 - x, \frac{1}{2} + y, \frac{3}{2} - z$; (ii) $1 - x, 1 - y, 1 - z$; (iii) $2 - x, 1 - y, 1 - z$.

Table 3
Hydrogen-bond geometry (Å, °) for **1**.

D—H$\cdots A$	D—H	H$\cdots A$	$D\cdots A$	D—H$\cdots A$
C2A—H2A$\cdots$Cl1^i	0.95	2.93	3.6784 (15)	137
C2B—H2B$\cdots$S1^{ii}	0.95	2.88	3.5459 (14)	128
C6B—H6BB$\cdots$S1^{iii}	0.99	2.97	3.9133 (13)	160

Symmetry codes: (i) $-x + 1, -y, -z + 1$; (ii) $x, -y + \frac{1}{2}, z - \frac{1}{2}$; (iii) $x, y + 1, z$.

Table 4
Short intermolecular contacts (Å) for **1**.

S1$\cdots$H6BB^i	2.967	H4B$\cdots$H3B^{iv}	2.230
Cl1$\cdots$H2A^{ii}	2.928	H4B$\cdots$H4B^{iv}	2.395
C1B$\cdots$C3A^{iii}	3.371	H1B$\cdots$H1CA^v	2.304
C1B$\cdots$H3A^{iii}	2.820	H2B$\cdots$S1^v	2.877
H4B$\cdots$C3B^{iv}	2.851	C2B$\cdots$H2CB^{vi}	2.847

Symmetry codes: (i) $x, -1 + y, z$; (ii) $1 - x, -y, 1 - z$; (iii) $1 - x, 1 - y, 1 - z$; (iv) $2 - x, 2 - y, 1 - z$; (v) $x, \frac{1}{2} - y, -\frac{1}{2} + z$; (vi) $x, \frac{3}{2} - y, -\frac{1}{2} + z$.

2. Structural commentary

Complex **1** crystallizes from methanol/n-butanol with NaOH as a base in the monoclinic space group $P2_1/n$ as a monomer (Fig. 1) instead of the dimer previously isolated from either methanol/benzene or methanol/ethyl acetate (Sturner *et al.*, 2024). The asymmetrically coordinated tetradentate organic ligand and one chloride provide a predominantly trigonal–bipyramidal coordination geometry (τ = 0.75; Table 1) to the metal ion (Addison *et al.*, 1984). The N1 and Cl1 atoms define the axial positions with a N1—Cd1—Cl1 bond angle of
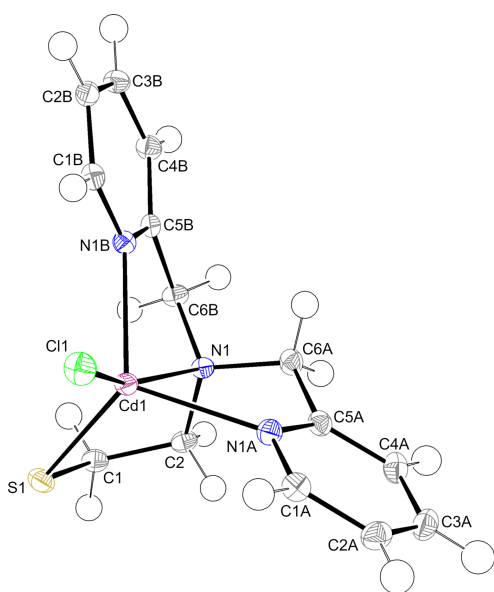
161.29 (3)°. The cadmium atom is 0.6107 (6) Å above the mean N1A–N1B–S1 trigonal plane, away from the axial N1 atom, and closer to the axial Cl1 atom. The three chelate rings have envelope conformations with either N1, C6A or C1 in the flap positions.

3. Supramolecular features

The packing of **1** is stabilized by π–π stacking interactions (Fig. 2; Table 2), hydrogen bonding (Fig. 3; Table 3) and van der Waals interactions (Table 4). One face of each ligand

Figure 1
The molecular structure of **1** with the atom-numbering scheme generated with *ORTEP-3 for Windows* (Farrugia, 2012). Displacement ellipsoids are drawn at the 50% probability level.
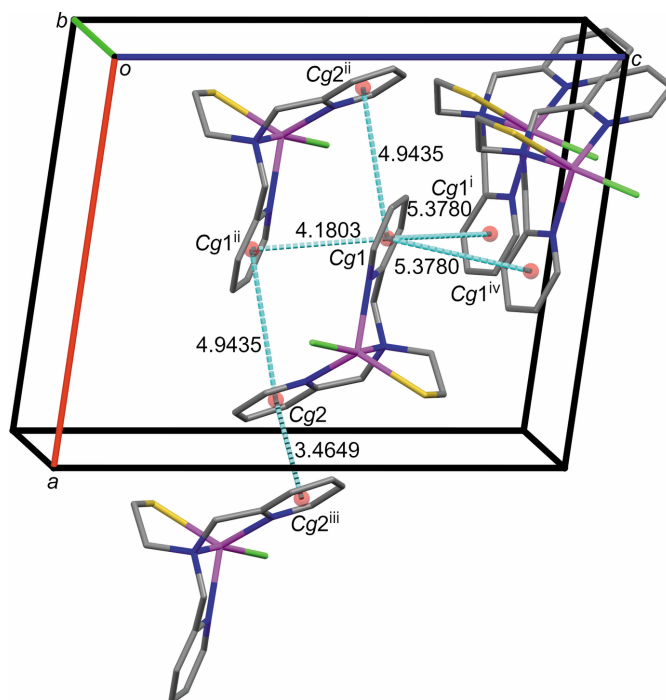
Figure 2
Centroid–centroid distances between nearby pyridyls in **1** viewed down the b axis illustrated using *Mercury* (Macrae *et al.*, 2020). Hydrogen atoms are omitted for clarity. Ring centroids are shown as red spheres. For additional numerical data, see Table 2. Symmetry codes: (i) $1 - x, \frac{1}{2} + y, \frac{3}{2} - z$; (ii) $1 - x, 1 - y, 1 - z$; (iii) $1 - x, -\frac{1}{2} + y, \frac{3}{2} - z$; (iv) $2 - x, 1 - y, 1 - z$.
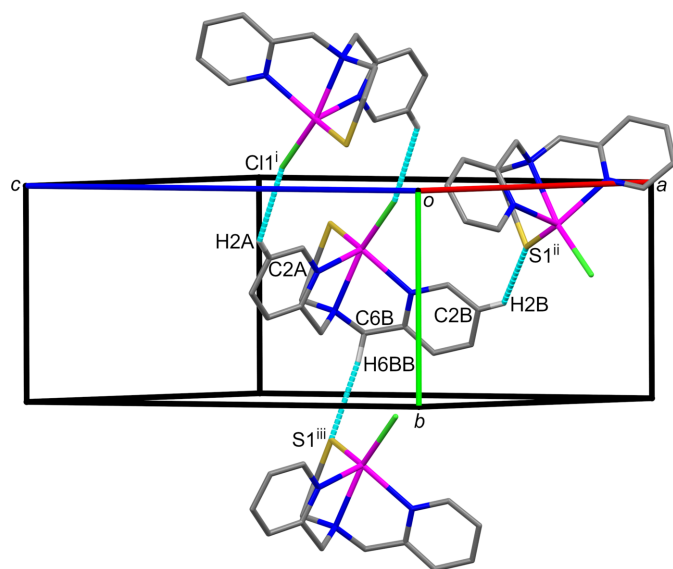
Figure 3
A view of the C—H···Cl and C—H···S hydrogen bonds in compound **1**, shown as cyan dashed lines illustrated using *Mercury* (Macrae *et al.*, 2020). Only hydrogen atoms involved in hydrogen bonds are shown for clarity. Symmetry codes as in Table 3.

pyridyl ring is stacked against an inversion-related equivalent with a small offset (Table 2), creating one-dimensional strands of molecules along the *a*-axis direction (Fig. 4). Interestingly, the N1*A* pyridyl rings have roughly 45° tilt angles and centroid–centroid distances of less than 5.5 Å with both the N1*B* pyridyl rings within the strands and N1*A* pyridyl rings of
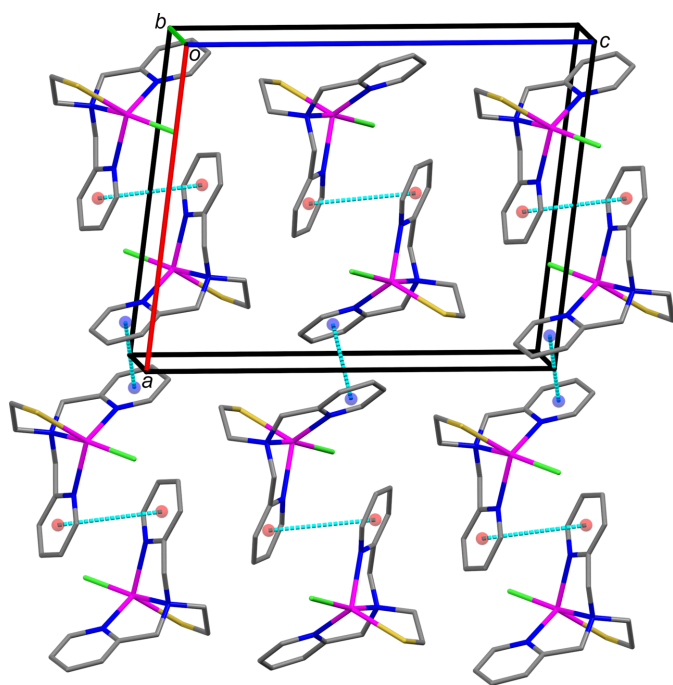

Figure 4
Offset parallel face-to-face π–π stacking interactions in **1** between the following ring centroids (*Cg*) shown as colored spheres: *Cg*1 (N1*A*/C1*A*–C5*A*, red sphere); *Cg*2 (N1*B*/C1*B*–C5*B*, blue sphere).

adjacent strands. Stabilizing contributions from these hybrid offset face-to-face/edge-to-face interactions are supported by a quantum chemistry study of the benzene dimer associating a tilt angle of about 45° with a shallow minimum on the path interconverting offset-parallel benzene dimers through a perpendicular saddle point (Jaffe & Smith, 1996). Furthermore, structural analysis of aromatic ligands bound to proteins found an abundance of phenylalanine and tyrosine residues with comparable ring orientation metrics (Brylinski, 2018).

Both metal-bound chlorine (Aullón *et al.*, 1998) and sulfur atoms (Chand *et al.*, 2020) serve as hydrogen-bond acceptors in **1**. Pairs of inversion-related molecules connected by C—H···Cl hydrogen bonds are stacked along the *b* axis. The C—H···S hydrogen bonds form sheets of molecules in the *bc* plane.

4. Hirshfeld surface analysis

Intermolecular interactions were investigated by quantitative analysis of the Hirshfeld surface and visualized with *Crystal-Explorer 21.5* (Spackman *et al.*, 2021). The Hirshfeld surface of
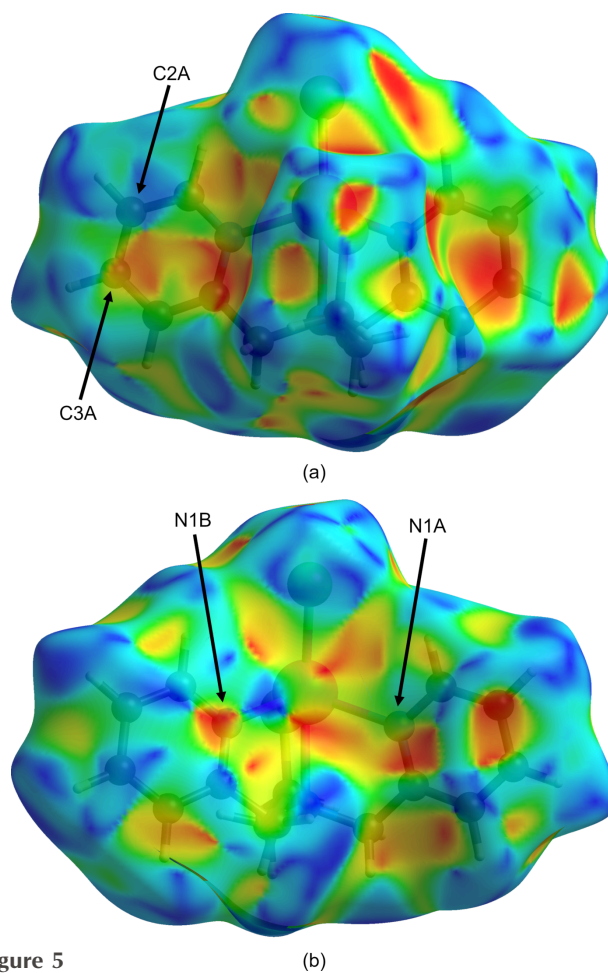

Figure 5
Hirshfeld surface of **1** plotted over the shape-index for two orientations generated with *Crystal Explorer 21.5* (Spackman *et al.*, 2021) with the ethylthiolato group to the (*a*) front and (*b*) back. Red and blue areas represent hollow and bump regions, respectively, on the shape-index surface.

1 plotted over the shape-index has hourglass figures associated with parallel face-to-face aromatic interactions over the C2*A*–C3*A* edge of the N1*A* pyridyl ring (Fig. 5*a*) and N1*B* atom (Fig. 5*b*). A pair of arc-shaped blue bumps associated with the periphery of the N1*B* pyridyl ring have complementary inversion-related red hollows surrounding the Cd—N1*A* bond (Fig. 5*b*). The blue-streaked dome associated with the chlorine atom nestles against the red hollow below the N1*B*—C5*B* bond (Fig. 5*b*).

The Hirshfeld surface of **1** mapped with the function d_{norm}, the sum of the distances from a surface point to the nearest interior (d_i) and exterior (d_e) atoms normalized by the van der Waals (vdW) radii of the corresponding atom (rvdW), is shown in Fig. 6. Contacts shorter than the sums of vdW radii are shown in red, those longer in blue, and those approximately equal as white areas. The most intense red spots correspond to close contacts between C3*B*, H3*B* and H4*B* along the pyridyl edges of inversion-related molecules
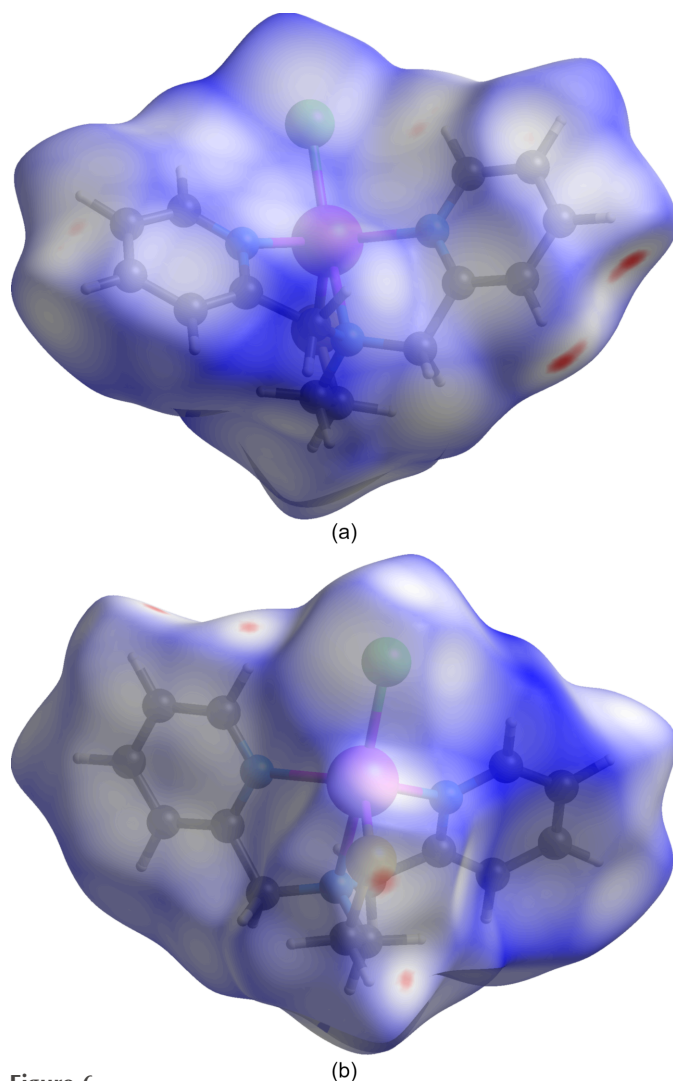

Figure 7
The full two-dimensional fingerprint plots for **1**, showing (*a*) all interactions, and components delineated into (*b*) H⋯H, (*c*) Cl⋯H/H⋯Cl, (*d*) C⋯H/H⋯C and (*e*) S⋯H/H⋯S interactions generated with *Crystal Explorer 21.5* (Spackman *et al.*, 2021). The d_i and d_e values are closest internal and external distances (in Å) from given points on the Hirshfeld surface.

(Fig. 6*a*). Atoms H1*B* and H2*B* of the same pyridyl ring form close contacts with H1*CA* and S1 of a single neighboring molecule (Fig. 6*b*). Additional faint spots associated with a close contact between C1*B* and both C3*A* and H3*A* are also observed (Fig. 6*a*). The remaining close contacts cause very faint red spots.

The overall 2D fingerprint plot for **1** is provided in Fig. 7*a*. Breakdown by element indicated H⋯H (51.2%) are predominant, followed by comparable amounts of Cl⋯H/H⋯Cl (13.9%), C⋯H/H⋯C (12.3%) and S⋯H/H⋯S (11.8%) interactions (Fig. 6*b*–*e*). Other minor contributions to the Hirshfeld surface are from N⋯C/C⋯N (3.8%), C⋯C (2.1%), Cl⋯C/C⋯Cl (2.0%), N⋯H/H⋯N (1.8%), Cd⋯H/H⋯Cd (0.7%), N⋯N (0.3%), and Cd⋯C/C⋯Cd (0.1%) contacts.

Figure 6
Views of the Hirshfeld surface of **1** plotted over normalized contact distance (d_{norm}) with the ethylthiolato group to the (*a*) back and (*b*) front. The plot was generated using *Crystal Explorer 21.5* (Spackman *et al.*, 2021) with d_{norm}.
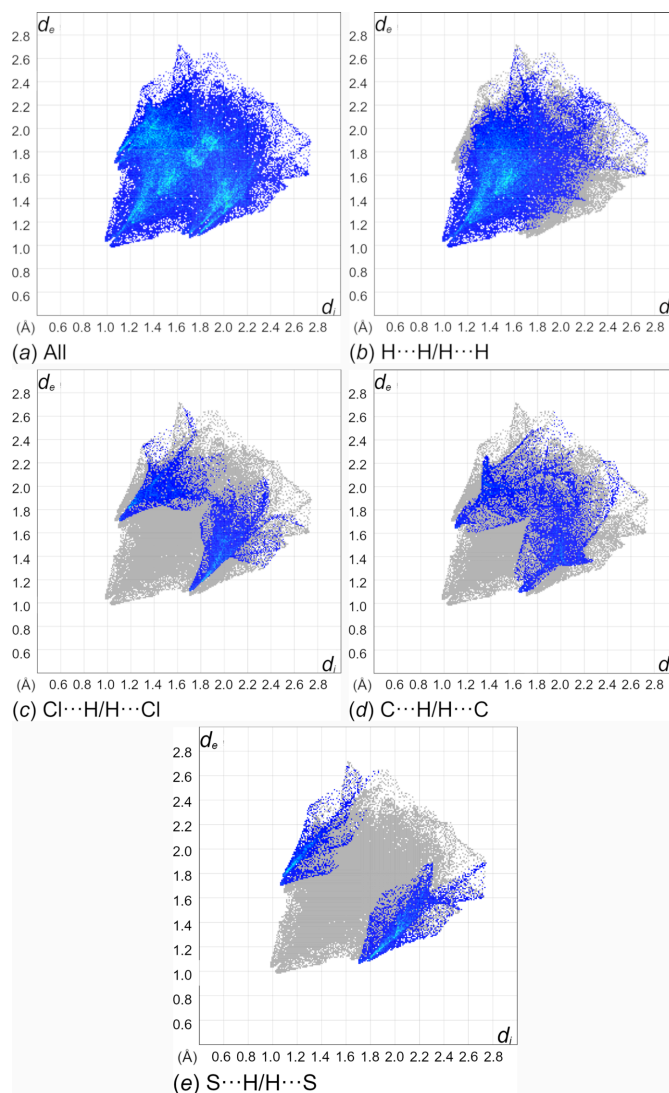
Table 5
Experimental details.

Crystal data	
Chemical formula	$[Cd(C_{14}H_{16}N_3S)Cl]$
M_r	406.21
Crystal system, space group	Monoclinic, $P2_1/c$
Temperature (K)	100
a, b, c (Å)	12.8451 (14), 7.4508 (7), 15.9284 (17)
β (°)	96.965 (3)
V (Å^3)	1513.2 (3)
Z	4
Radiation type	Mo $K\alpha$
μ (mm^{-1})	1.75
Crystal size (mm)	$0.37 \times 0.31 \times 0.24$
Data collection	
Diffractometer	Bruker D8 Venture Photon 3
Absorption correction	Multi-scan (*SADABS*; Krause *et al.*, 2015)
T_{min}, T_{max}	0.815, 1.000
No. of measured, independent and observed [$I > 2\sigma(I)$] reflections	209395, 3747, 3658
R_{int}	0.039
$(\sin\theta/\lambda)_{max}$ (Å^{-1})	0.667
Refinement	
$R[F^2 > 2\sigma(F^2)]$, $wR(F^2)$, S	0.015, 0.035, 1.08
No. of reflections	3747
No. of parameters	181
H-atom treatment	H-atom parameters constrained
$\Delta\rho_{max}, \Delta\rho_{min}$ (e Å^{-3})	0.40, −0.41

Computer programs: *APEX5* (Bruker, 2023), *SAINT-Plus* (Bruker, 2012), *SHELXS2014/5* (Sheldrick, 2015*a*), *SHELXL2014/5* (Sheldrick, 2015*b*), *ShelXle* (Hübschle *et al.*, 2011), *ORTEP-3 for Windows* (Farrugia, 2012), *Mercury* (Macrae *et al.*, 2020), *CrystalExplorer* (Spackman *et al.*, 2021), *OLEX2* (Dolomanov *et al.*, 2009), *PLATON* (Spek, 2020), and *publCIF* (Westrip, 2010).

5. Database survey

A search of the Cambridge Structural Database (CSD, Version 5.45, update of June 2024; Groom *et al.*, 2016) for complexes of cadmium bound to a thiolate sulfur, three nitrogen and one chlorine atoms yielded ten hits, all of which included μ_2-Cl bridges between cadmium atoms. Three of the complexes are solvomorphs of the μ_2-Cl$_2$ bridged dimer [CdLCl]$_2$ (refcodes BOJTIH, BOJTUT, BOJVAB: Sturner *et al.*, 2024). Other μ_2-Cl$_2$ bridged dimers included bis(μ_2-chlorido)bis(2,2′-bipyridine-*N*,*N*′)bis(4,6-dimethylpyrimidine-2-thiolato-*N*,*S*)dicadmium(II) and bis(μ_2-chlorido)bis(4,6-dimethylpyrimidine-2-thiolato-*N*,*S*)bis(1,10-phenanthroline-*N*,*N*′)dicadmium(II) with N$_3$SCl$_2$ metal coordination environments (refcodes LUMZOJ and LUMZUP, respectively: Lang *et al.*, 2009). Four of the structurally characterized complexes were μ_2-Cl bridged complexes of *N*-alkylated hexaazadithiophenolate dinucleating macrocycles (refcode FIMKOC: Lozan & Kersting, 2005; refcodes KEVXIT, KEVXOZ and KEVXUF: Gressenbuch & Kersting, 2007). The final complex was the 1D polymer $\{[Cd_3(deatrz)_4Cl_2(SCN)_4]\cdot 2H_2O\}_n$ (deatrz = 3,5-diethyl-4-amino-1,2,4-triazole) constructed of trinuclear cadmium units bridged by both triazole ligands and chloride (refcode EQUHAZ: Yi *et al.*, 2004).

A further search of the CSD for complexes of Cd^{2+} bound to chelating ligands containing both an aromatic amine and an alkylthiolate yielded one binuclear complex (Sturner *et al.*, 2024) and multinuclear complexes [CdL]$_3$(ClO$_4$)$_3$ (refcode BERXUV: Brennan *et al.*, 2022) and bis(μ_3-carbonato)hexakis{μ_2-*N*-(2-pyridylmethyl)-*N*-[2-(methylthio)ethyl]-*N*-(2-mercaptoethyl)amine}hexacadmium(II) diperchlorate monohydrate (refcode DEZCUI: Lai *et al.*, 2013). Additional reported Cd^{2+} complexes containing separate aromatic amine and alkyl thiolate ligands included bis(3,5-dimethylpyridine)-bis(triphenylmethanethiolato)cadmium(II) (refcode HABQEJ: Rheingold & Hampden-Smith, 2015), *catena*-[bis-(μ_2-5,10,15,20-tetrakis(4-pyridyl)porphyrinato)bis(μ_2-2-mercaptoethanol)dicadmium(II) dimethylformamide solvate] (refcode JITFEY: Zheng *et al.*, 2007), bis(μ_2-oxo-2-ethoxyethanethiolato)bis(2,2′-bipyridine)diiodidodicadmium(II) (refcode OJEPOK: Clegg & Fraser, 2016) and bis(μ_2-oxo-2-ethoxyethanethiolato)bis(2,2′-bipyridine)dibromidodicadmium(II) (refcode OJEPUQ: Clegg & Fraser, 2016).

6. Synthesis and crystallization

Literature procedures were used to prepare **LH** (Lai *et al.*, 2013). One equivalent of 50 m*M* of CdCl$_2$ in methanol was added dropwise with stirring to a 50 m*M* solution of **LH** in methanol containing one equivalent of NaOH. *n*-Butanol was added as a cosolvent. After four weeks of slow evaporation, colorless X-ray quality blocks of **1** were obtained.

7. Refinement

Crystal data, data collection and structure refinement details are summarized in Table 5. The hydrogen atoms were placed in calculated positions with C—H distances of 0.95 Å (aromatic) and 0.99 Å (methylene) and refined as riding atoms with $U_{iso}(H) = 1.2U_{eq}(C)$.

References

Addison, A. W., Rao, T. N., Reedijk, J., van Rijn, J. & Verschoor, G. C. (1984). *J. Chem. Soc. Dalton Trans.* pp. 1349–1356.
Aullón, G., Bellamy, D., Guy Orpen, A., Brammer, L. & Bruton, E. A. (1998). *Chem. Commun.* pp. 653–654.
Brennan, H. M., Bunde, S. G., Kuang, Q., Palomino, T. V., Sacks, J. S., Berry, S. M., Butcher, R. J., Poutsma, J. C., Pike, R. D. & Bebout, D. C. (2022). *Inorg. Chem.* **61**, 19857–19869.
Bruker (2012). *SAINT-Plus*. Bruker AXS Inc. Madison, Wisconsin, USA.
Bruker (2023). *APEX5*. Bruker AXS Inc. Madison, Wisconsin, USA.

research communications

Brylinski, M. (2018). *Chem. Biol. Drug Des.* **91**, 380–390.

Chand, A., Sahoo, D. K., Rana, A., Jena, S. & Biswal, H. S. (2020). *Acc. Chem. Res.* **53**, 1580–1592.

Clegg, W. & Fraser, K. A. (2016). *CSD Communication* (refcode OJEPOK). CCDC, Cambridge, England.

Dolomanov, O. V., Bourhis, L. J., Gildea, R. J., Howard, J. A. K. & Puschmann, H. (2009). *J. Appl. Cryst.* **42**, 339–341.

Farrugia, L. J. (2012). *J. Appl. Cryst.* **45**, 849–854.

Gressenbuch, M. & Kersting, B. (2007). *Eur. J. Inorg. Chem.* pp. 90–102.

Groom, C. R., Bruno, I. J., Lightfoot, M. P. & Ward, S. C. (2016). *Acta Cryst.* B**72**, 171–179.

Hübschle, C. B., Sheldrick, G. M. & Dittrich, B. (2011). *J. Appl. Cryst.* **44**, 1281–1284.

Jaffe, R. L. & Smith, G. D. (1996). *J. Chem. Phys.* **105**, 2780–2788.

Krause, L., Herbst-Irmer, R., Sheldrick, G. M. & Stalke, D. (2015). *J. Appl. Cryst.* **48**, 3–10.

Lai, W., Berry, S. M., Kaplan, W. P., Hain, M. S., Poutsma, J. C., Butcher, R. J., Pike, R. D. & Bebout, D. C. (2013). *Inorg. Chem.* **52**, 2286–2288.

Lane, T. W. & Morel, F. M. M. (2000). *Proc. Natl Acad. Sci. USA*, **97**, 4627–4631.

Lang, E. S., Stieler, R. & de Oliveira, G. M. (2009). *Polyhedron*, **28**, 3844–3848.

Lozan, V. & Kersting, B. (2005). *Eur. J. Inorg. Chem.* pp. 504–512.

Macrae, C. F., Sovago, I., Cottrell, S. J., Galek, P. T. A., McCabe, P., Pidcock, E., Platings, M., Shields, G. P., Stevens, J. S., Towler, M. & Wood, P. A. (2020). *J. Appl. Cryst.* **53**, 226–235.

Rheingold, A. L. & Hampden-Smith, M. (2015). *CSD Communication* (refcode HABQEJ). CCDC, Cambridge, England.

Sheldrick, G. M. (2015a). *Acta Cryst.* A**71**, 3–8.

Sheldrick, G. M. (2015b). *Acta Cryst.* C**71**, 3–8.

Spackman, P. R., Turner, M. J., McKinnon, J. J., Wolff, S. K., Grimwood, D. J., Jayatilaka, D. & Spackman, M. A. (2021). *J. Appl. Cryst.* **54**, 1006–1011.

Spek, A. L. (2020). *Acta Cryst.* E**76**, 1–11.

Sturner, M. A., Thomas, I. D., Owusu-Koramoah, J., Reynolds, T. M., Berry, S. M., Butcher, R. J. & Bebout, D. C. (2024). *New J. Chem.* **48**, 2547–2557.

Westrip, S. P. (2010). *J. Appl. Cryst.* **43**, 920–925.

Xu, Y., Feng, L., Jeffrey, P. D., Shi, Y. & Morel, F. M. M. (2008). *Nature*, **452**, 56–61.

Yi, L., Ding, B., Zhao, B., Cheng, P., Liao, D., Yan, S. & Jiang, Z. (2004). *Inorg. Chem.* **43**, 33–43.

Zheng, N., Zhang, J., Bu, X. & Feng, P. (2007). *Cryst. Growth Des.* **7**, 2576–2581.

Crystal structure and Hirshfeld surface analysis of {2-[bis(pyridin-2-ylmethyl)-amino]ethane-1-thiolato}chloridocadmium(II)

Todd M. Reynolds, Steven M. Berry and Deborah C. Bebout

Computing details

{2-[Bis(pyridin-2-ylmethyl)amino]ethane-1-thiolato}chloridocadmium(II)

Crystal data

[Cd(C$_{14}$H$_{16}$N$_3$S)Cl]	$F(000) = 808$
$M_r = 406.21$	$D_x = 1.783$ Mg m^{-3}
Monoclinic, $P2_1/c$	Mo $K\alpha$ radiation, $\lambda = 0.71073$ Å
$a = 12.8451$ (14) Å	Cell parameters from 9498 reflections
$b = 7.4508$ (7) Å	$\theta = 2.6–28.3°$
$c = 15.9284$ (17) Å	$\mu = 1.75$ mm^{-1}
$\beta = 96.965$ (3)°	$T = 100$ K
$V = 1513.2$ (3) Å^3	Block, colourless
$Z = 4$	$0.37 \times 0.31 \times 0.24$ mm

Data collection

Bruker D8 Venture Photon 3 diffractometer	209395 measured reflections
Radiation source: Imus	3747 independent reflections
Multi-layer optics monochromator	3658 reflections with $I > 2\sigma(I)$
ω and ψ scans	$R_{int} = 0.039$
Absorption correction: multi-scan (*SADABS*; Krause *et al.*, 2015)	$\theta_{max} = 28.3°$, $\theta_{min} = 2.6°$
$T_{min} = 0.815$, $T_{max} = 1.000$	$h = -17 \rightarrow 17$
	$k = -9 \rightarrow 9$
	$l = -21 \rightarrow 21$

Refinement

Refinement on F^2	Hydrogen site location: inferred from neighbouring sites
Least-squares matrix: full	H-atom parameters constrained
$R[F^2 > 2\sigma(F^2)] = 0.015$	$w = 1/[\sigma^2(F_o^2) + (0.0072P)^2 + 1.2877P]$
$wR(F^2) = 0.035$	where $P = (F_o^2 + 2F_c^2)/3$
$S = 1.08$	$(\Delta/\sigma)_{max} = 0.003$
3747 reflections	$\Delta\rho_{max} = 0.40$ e Å^{-3}
181 parameters	$\Delta\rho_{min} = -0.41$ e Å^{-3}
0 restraints	
Primary atom site location: other	

Special details

Geometry. All esds (except the esd in the dihedral angle between two l.s. planes) are estimated using the full covariance matrix. The cell esds are taken into account individually in the estimation of esds in distances, angles and torsion angles; correlations between esds in cell parameters are only used when they are defined by crystal symmetry. An approximate (isotropic) treatment of cell esds is used for estimating esds involving l.s. planes.

Fractional atomic coordinates and isotropic or equivalent isotropic displacement parameters (Å²)

	x	*y*	*z*	U_{iso}*/U_{eq}
Cd1	0.74709 (2)	0.31187 (2)	0.58883 (2)	0.01483 (3)
Cl1	0.70287 (3)	0.08478 (4)	0.47746 (2)	0.02385 (7)
S1	0.84107 (3)	0.20129 (4)	0.72345 (2)	0.02084 (7)
N1	0.75863 (8)	0.60172 (14)	0.66540 (6)	0.0154 (2)
N1A	0.57698 (8)	0.41020 (15)	0.59984 (7)	0.0183 (2)
N1B	0.83627 (8)	0.51728 (14)	0.51512 (6)	0.01542 (19)
C1A	0.49427 (11)	0.29875 (19)	0.58949 (9)	0.0208 (3)
H1A	0.501646	0.186315	0.562702	0.025*
C1B	0.86110 (10)	0.48024 (17)	0.43735 (8)	0.0172 (2)
H1B	0.838155	0.369821	0.411608	0.021*
C1C	0.85864 (10)	0.41625 (18)	0.77926 (8)	0.0199 (2)
H1CA	0.863686	0.393122	0.840820	0.024*
H1CB	0.926067	0.469376	0.767630	0.024*
C2A	0.39857 (11)	0.3412 (2)	0.61632 (9)	0.0236 (3)
H2A	0.341147	0.260232	0.607530	0.028*
C2B	0.91853 (10)	0.59597 (18)	0.39343 (8)	0.0185 (2)
H2B	0.936190	0.565033	0.339052	0.022*
C2C	0.77164 (10)	0.55322 (18)	0.75572 (8)	0.0180 (2)
H2CA	0.704677	0.503679	0.770438	0.022*
H2CB	0.787401	0.663183	0.789789	0.022*
C3A	0.38858 (10)	0.5042 (2)	0.65621 (9)	0.0254 (3)
H3A	0.324587	0.535668	0.676714	0.030*
C3B	0.94985 (10)	0.75858 (19)	0.43059 (8)	0.0211 (2)
H3B	0.989827	0.841014	0.402160	0.025*
C4A	0.47328 (10)	0.6211 (2)	0.66585 (9)	0.0225 (3)
H4A	0.467619	0.734369	0.692343	0.027*
C4B	0.92207 (10)	0.79909 (17)	0.50963 (8)	0.0193 (2)
H4B	0.940726	0.911505	0.535305	0.023*
C5A	0.56633 (10)	0.57087 (18)	0.63637 (8)	0.0179 (2)
C5B	0.86663 (9)	0.67381 (16)	0.55110 (8)	0.0148 (2)
C6A	0.65923 (10)	0.69587 (17)	0.64093 (8)	0.0188 (2)
H6AA	0.661166	0.753150	0.585060	0.023*
H6AB	0.650871	0.791863	0.682566	0.023*
C6B	0.84680 (10)	0.70666 (17)	0.64152 (8)	0.0174 (2)
H6BA	0.910811	0.675772	0.679852	0.021*
H6BB	0.832371	0.835846	0.648930	0.021*

Atomic displacement parameters (Å²)

	U^{11}	U^{22}	U^{33}	U^{12}	U^{13}	U^{23}
Cd1	0.01714 (5)	0.01179 (5)	0.01600 (5)	−0.00086 (3)	0.00376 (3)	−0.00072 (3)
Cl1	0.03070 (16)	0.01655 (14)	0.02427 (15)	−0.00161 (12)	0.00322 (12)	−0.00640 (11)
S1	0.02707 (16)	0.01780 (15)	0.01783 (14)	0.00230 (12)	0.00344 (12)	0.00358 (11)
N1	0.0162 (5)	0.0151 (5)	0.0152 (5)	−0.0013 (4)	0.0032 (4)	−0.0003 (4)
N1A	0.0181 (5)	0.0178 (5)	0.0191 (5)	−0.0005 (4)	0.0028 (4)	−0.0011 (4)
N1B	0.0163 (5)	0.0145 (5)	0.0154 (5)	−0.0001 (4)	0.0015 (4)	0.0000 (4)
C1A	0.0200 (6)	0.0215 (6)	0.0209 (6)	−0.0024 (5)	0.0019 (5)	−0.0014 (5)
C1B	0.0176 (5)	0.0172 (6)	0.0163 (5)	0.0012 (4)	0.0001 (4)	−0.0018 (4)
C1C	0.0220 (6)	0.0219 (6)	0.0157 (5)	−0.0015 (5)	0.0019 (4)	0.0012 (5)
C2A	0.0172 (6)	0.0301 (7)	0.0231 (6)	−0.0033 (5)	0.0007 (5)	0.0014 (5)
C2B	0.0176 (5)	0.0229 (6)	0.0153 (5)	0.0027 (5)	0.0026 (4)	0.0005 (5)
C2C	0.0201 (6)	0.0206 (6)	0.0140 (5)	−0.0028 (5)	0.0044 (4)	−0.0020 (5)
C3A	0.0158 (6)	0.0361 (8)	0.0243 (6)	0.0033 (5)	0.0023 (5)	0.0002 (6)
C3B	0.0215 (6)	0.0218 (6)	0.0206 (6)	−0.0025 (5)	0.0050 (5)	0.0044 (5)
C4A	0.0199 (6)	0.0246 (7)	0.0226 (6)	0.0056 (5)	0.0015 (5)	−0.0031 (5)
C4B	0.0220 (6)	0.0157 (6)	0.0206 (6)	−0.0027 (5)	0.0035 (5)	0.0001 (5)
C5A	0.0178 (6)	0.0189 (6)	0.0168 (5)	0.0016 (5)	0.0011 (4)	0.0000 (5)
C5B	0.0141 (5)	0.0145 (5)	0.0158 (5)	0.0011 (4)	0.0015 (4)	0.0004 (4)
C6A	0.0196 (6)	0.0148 (6)	0.0222 (6)	0.0016 (4)	0.0031 (5)	−0.0013 (5)
C6B	0.0210 (6)	0.0156 (6)	0.0163 (5)	−0.0051 (5)	0.0045 (4)	−0.0022 (4)

Geometric parameters (Å, °)

Cd1—N1A	2.3313 (11)	C2A—C3A	1.384 (2)
Cd1—N1B	2.3151 (11)	C2A—H2A	0.9500
Cd1—N1	2.4758 (11)	C2B—C3B	1.3865 (19)
Cd1—S1	2.4710 (4)	C2B—H2B	0.9500
Cd1—Cl1	2.4674 (4)	C2C—H2CA	0.9900
S1—C1C	1.8324 (14)	C2C—H2CB	0.9900
N1—C6B	1.4639 (15)	C3A—C4A	1.388 (2)
N1—C6A	1.4676 (16)	C3A—H3A	0.9500
N1—C2C	1.4730 (15)	C3B—C4B	1.3828 (18)
N1A—C1A	1.3427 (17)	C3B—H3B	0.9500
N1A—C5A	1.3452 (17)	C4A—C5A	1.3876 (18)
N1B—C5B	1.3366 (16)	C4A—H4A	0.9500
N1B—C1B	1.3447 (16)	C4B—C5B	1.3889 (17)
C1A—C2A	1.3862 (19)	C4B—H4B	0.9500
C1A—H1A	0.9500	C5A—C6A	1.5085 (18)
C1B—C2B	1.3792 (18)	C5B—C6B	1.5126 (17)
C1B—H1B	0.9500	C6A—H6AA	0.9900
C1C—C2C	1.5261 (18)	C6A—H6AB	0.9900
C1C—H1CA	0.9900	C6B—H6BA	0.9900
C1C—H1CB	0.9900	C6B—H6BB	0.9900
N1A—Cd1—N1B	110.87 (4)	C1B—C2B—H2B	120.8

N1A—Cd1—N1	71.91 (4)	C3B—C2B—H2B	120.8
N1A—Cd1—S1	113.78 (3)	N1—C2C—C1C	113.39 (10)
N1A—Cd1—Cl1	97.67 (3)	N1—C2C—H2CA	108.9
N1B—Cd1—N1	70.70 (4)	C1C—C2C—H2CA	108.9
N1B—Cd1—S1	116.16 (3)	N1—C2C—H2CB	108.9
N1B—Cd1—Cl1	100.00 (3)	C1C—C2C—H2CB	108.9
S1—Cd1—N1	82.51 (3)	H2CA—C2C—H2CB	107.7
Cl1—Cd1—N1	161.29 (3)	C2A—C3A—C4A	119.13 (13)
Cl1—Cd1—S1	116.159 (13)	C2A—C3A—H3A	120.4
C1C—S1—Cd1	98.51 (4)	C4A—C3A—H3A	120.4
C6B—N1—C6A	110.56 (10)	C4B—C3B—C2B	119.07 (12)
C6B—N1—C2C	112.65 (10)	C4B—C3B—H3B	120.5
C6A—N1—C2C	111.64 (10)	C2B—C3B—H3B	120.5
C6B—N1—Cd1	109.87 (7)	C5A—C4A—C3A	119.27 (13)
C6A—N1—Cd1	106.73 (7)	C5A—C4A—H4A	120.4
C2C—N1—Cd1	105.07 (7)	C3A—C4A—H4A	120.4
C1A—N1A—C5A	118.89 (11)	C3B—C4B—C5B	119.35 (12)
C1A—N1A—Cd1	122.09 (9)	C3B—C4B—H4B	120.3
C5A—N1A—Cd1	117.23 (8)	C5B—C4B—H4B	120.3
C5B—N1B—C1B	118.99 (11)	N1A—C5A—C4A	121.57 (12)
C5B—N1B—Cd1	119.73 (8)	N1A—C5A—C6A	116.68 (11)
C1B—N1B—Cd1	121.25 (8)	C4A—C5A—C6A	121.72 (12)
N1A—C1A—C2A	122.62 (13)	N1B—C5B—C4B	121.48 (11)
N1A—C1A—H1A	118.7	N1B—C5B—C6B	118.39 (11)
C2A—C1A—H1A	118.7	C4B—C5B—C6B	119.96 (11)
N1B—C1B—C2B	122.69 (12)	N1—C6A—C5A	112.04 (10)
N1B—C1B—H1B	118.7	N1—C6A—H6AA	109.2
C2B—C1B—H1B	118.7	C5A—C6A—H6AA	109.2
C2C—C1C—S1	114.95 (9)	N1—C6A—H6AB	109.2
C2C—C1C—H1CA	108.5	C5A—C6A—H6AB	109.2
S1—C1C—H1CA	108.5	H6AA—C6A—H6AB	107.9
C2C—C1C—H1CB	108.5	N1—C6B—C5B	112.70 (10)
S1—C1C—H1CB	108.5	N1—C6B—H6BA	109.1
H1CA—C1C—H1CB	107.5	C5B—C6B—H6BA	109.1
C3A—C2A—C1A	118.48 (13)	N1—C6B—H6BB	109.1
C3A—C2A—H2A	120.8	C5B—C6B—H6BB	109.1
C1A—C2A—H2A	120.8	H6BA—C6B—H6BB	107.8
C1B—C2B—C3B	118.37 (12)		
C5A—N1A—C1A—C2A	−1.2 (2)	C3A—C4A—C5A—N1A	−1.1 (2)
Cd1—N1A—C1A—C2A	163.14 (10)	C3A—C4A—C5A—C6A	176.77 (12)
C5B—N1B—C1B—C2B	1.21 (18)	C1B—N1B—C5B—C4B	0.69 (18)
Cd1—N1B—C1B—C2B	−176.79 (9)	Cd1—N1B—C5B—C4B	178.72 (9)
Cd1—S1—C1C—C2C	31.48 (9)	C1B—N1B—C5B—C6B	−174.55 (11)
N1A—C1A—C2A—C3A	−0.8 (2)	Cd1—N1B—C5B—C6B	3.49 (14)
N1B—C1B—C2B—C3B	−1.37 (19)	C3B—C4B—C5B—N1B	−2.37 (19)
C6B—N1—C2C—C1C	−69.38 (14)	C3B—C4B—C5B—C6B	172.79 (12)
C6A—N1—C2C—C1C	165.53 (10)	C6B—N1—C6A—C5A	160.44 (10)

Cd1—N1—C2C—C1C	50.21 (11)	C2C—N1—C6A—C5A	−73.31 (13)
S1—C1C—C2C—N1	−59.72 (13)	Cd1—N1—C6A—C5A	40.98 (11)
C1A—C2A—C3A—C4A	1.8 (2)	N1A—C5A—C6A—N1	−42.59 (15)
C1B—C2B—C3B—C4B	−0.36 (19)	C4A—C5A—C6A—N1	139.47 (12)
C2A—C3A—C4A—C5A	−0.9 (2)	C6A—N1—C6B—C5B	−85.38 (13)
C2B—C3B—C4B—C5B	2.2 (2)	C2C—N1—C6B—C5B	148.94 (11)
C1A—N1A—C5A—C4A	2.09 (19)	Cd1—N1—C6B—C5B	32.17 (12)
Cd1—N1A—C5A—C4A	−162.98 (10)	N1B—C5B—C6B—N1	−25.47 (16)
C1A—N1A—C5A—C6A	−175.86 (12)	C4B—C5B—C6B—N1	159.22 (11)
Cd1—N1A—C5A—C6A	19.08 (14)		

Hydrogen-bond geometry (Å, º)

D—H⋯A	D—H	H⋯A	D⋯A	D—H⋯A
C2A—H2A⋯Cl1[i]	0.95	2.93	3.6784 (15)	137
C2B—H2B⋯S1[ii]	0.95	2.88	3.5459 (14)	128
C6B—H6BB⋯S1[iii]	0.99	2.97	3.9133 (13)	160

Symmetry codes: (i) −x+1, −y, −z+1; (ii) x, −y+1/2, z−1/2; (iii) x, y+1, z.